THE JOURNAL OF BIOLOGICAL CHEMISTRY VOL. 283, NO. 39, pp. 26684–26693, September 26, 2008

Retinopathy in Mice Induced by Disrupted All-*trans*-retinal Clearance*[S]

Received for publication, June 12, 2008, and in revised form, July 16, 2008 Published, JBC Papers in Press, July 25, 2008, DOI 10.1074/jbc.M804505200

Akiko Maeda[‡], Tadao Maeda[‡§], Marcin Golczak[‡], and Krzysztof Palczewski[‡1]

From the [‡]Department of Pharmacology and [§]Department of Ophthalmology, Case Western Reserve University, Cleveland, Ohio 44106

The visual (retinoid) cycle is a fundamental metabolic process in vertebrate retina responsible for production of 11-*cis*-retinal, the chromophore of rhodopsin and cone pigments. 11-*cis*-Retinal is bound to opsins, forming visual pigments, and when the resulting visual chromophore 11-*cis*-retinylidene is photoisomerized to all-*trans*-retinylidene, all-*trans*-retinal is released from these receptors. Toxic byproducts of the visual cycle formed from all-*trans*-retinal often are associated with lipofuscin deposits in the retinal pigmented epithelium (RPE), but it is not clear whether aberrant reactions of the visual cycle participate in RPE atrophy, leading to a rapid onset of retinopathy. Here we report that mice lacking both the ATP-binding cassette transporter 4 (Abca4) and enzyme retinol dehydrogenase 8 (Rdh8), proteins critical for all-*trans*-retinal clearance from photoreceptors, developed severe RPE/photoreceptor dystrophy at an early age. This phenotype includes lipofuscin, drusen, and basal laminar deposits, Bruch's membrane thickening, and choroidal neovascularization. Importantly, the severity of visual dysfunction and retinopathy was exacerbated by light but attenuated by treatment with retinylamine, a visual cycle inhibitor that slows the flow of all-*trans*-retinal through the visual cycle. These findings provide direct evidence that aberrant production of toxic condensation byproducts of the visual cycle in mice can lead to rapid, progressive retinal degeneration.

What discriminates the eye from other organs is its light sensitivity and associated metabolic transformations that restore the light-sensitive chromophore (1). It is unclear if aberrations in the visual cycle and byproduct accumulation could be an underlying cause of retinopathy or merely a nonspecific nonpathogenic reflection of impaired metabolism. To distinguish between these two possibilities, we disrupted two genes critical for clearance of light-generated all-*trans*-retinal from rhodopsin and cone visual pigments (2, 3). Both the photoreceptor-specific ATP-binding cassette transporter (ABCA4) (4) and all-*trans*-retinol dehydrogenases (RDHs)[2] are involved in removal of all-*trans*-retinal from photoreceptors (5) (Scheme 1).

ABCA4, also known as ABCR or the rim protein, localizes to the rim of photoreceptor discs and transfers all-*trans*-retinal from the inside to the outside of disc membranes once all-*trans*-retinal is released from visual pigments (4). Diretinoid-pyridinium-ethanolamine (A2E) (6, 7) and retinal dimer (RALdi) conjugates (8) are the major fluorophores of lipofuscins produced from all-*trans*-retinal. Even in the presence of a functional transporter, both A2E and RALdi can accumulate as a consequence of aging (9) and produce toxic effects on RPE cells (10, 11). Patients affected by age-related macular degeneration (AMD), Stargardt disease with a disabled *ABCA4* gene, or other retinal diseases associated with lipofuscin accumulation develop retinal degeneration. ABCA4 mutations also are linked with a high risk of AMD (12). However, no such degeneration was observed in $Abca4^{-/-}$ mice, although RPE atrophy was detected (4, 13, 14). Thus, the mouse and human do not evidence identical phenotypic responses to fluorophore accumulation.

RDH8 is one of the main enzymes that reduces all-*trans*-retinal in rod and cone outer segments (ROS/COS) (5). In $Rdh8^{-/-}$ mice, all-*trans*-retinal could form lipofuscin toxins in the cytoplasm of ROS/COS, as seen in $Abca4^{-/-}$ mice. But the abnormal physiological responses and pathology observed in $Rdh8^{-/-}$ mice were even milder than the effects seen in $Abca4^{-/-}$ mice, and only modest all-*trans*-retinal condensation to A2E was observed (15). RDH8 mutations have yet to be associated with any inherited retinal diseases of humans.

Here, we report that mice carrying a double knock-out of the *Rdh8* and *Abca4* genes rapidly accumulated all-*trans*-retinal condensation products and exhibited accentuated RPE/photoreceptor dystrophy at an early age. These observations link abnormal function of the visual cycle to RPE/photoreceptor degeneration. The described double mutant mice with disrupted all-*trans*-retinal clearance should serve as a superior model to increase understanding of the molecular mechanisms involved in retinal dysfunction and pathology. Moreover, these double knock-out mice will allow the design and testing of

* This work was supported, in whole or in part, by National Institutes of Health Grants EY09339, P30 EY11373, and EY08123. The costs of publication of this article were defrayed in part by the payment of page charges. This article must therefore be hereby marked "*advertisement*" in accordance with 18 U.S.C. Section 1734 solely to indicate this fact.

[S] The on-line version of this article (available at http://www.jbc.org) contains supplemental Fig. S1.

[1] To whom correspondence should be addressed: Dept. of Pharmacology, School of Medicine, Case Western Reserve University, 10900 Euclid Ave., Cleveland, OH 44106-4965. Tel.: 216-368-4631; Fax: 216-368-1300; E-mail: kxp65@case.edu.

[2] The abbreviations used are: RDH, retinol dehydrogenase; AMD, age-related macular degeneration; A2E, diretinoid-pyridinium-ethanolamine; A2PE, diretinoid-pyridinium-phosphatidylethanolamine; RALdi, all-*trans*-retinal dimer; ROS, rod outer segment(s); RPE, retinal pigmented epithelium; VEGF, vascular endothelial growth factor; WT, wild type; COS, cone outer segment(s); HPLC, high pressure liquid chromatography; ERG, electroretinogram; DAPI, 4′,6-diamidino-2-phenylindole; PNA, peanut agglutinin lectin.

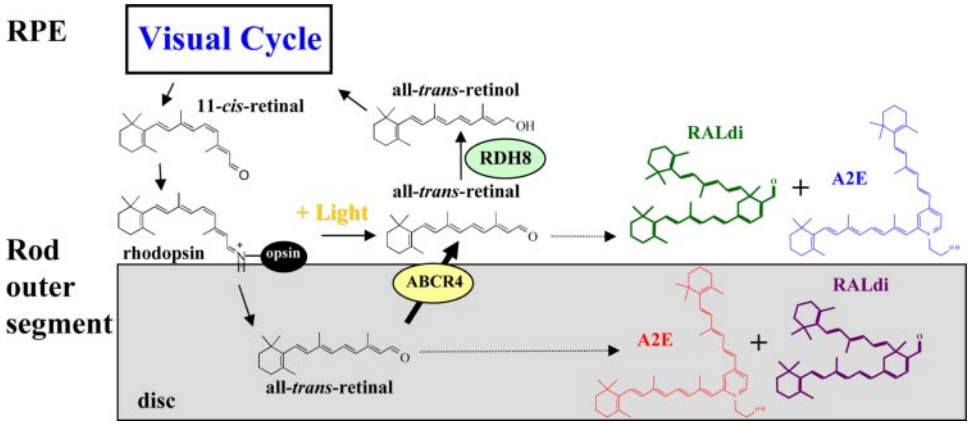

SCHEME 1. **Retinoid flow in the visual cycle and condensation of all-*trans*-retinal.** After 11-*cis*-retinal is bound to opsin forming rhodopsin, the resulting visual chromophore 11-*cis*-retinylidene is photoisomerized to all-*trans*-retinylidene, the precursor of all-*trans*-retinal. Most of the all-*trans*-retinal dissociates from opsin into the cytoplasm, where it is reduced to all-*trans*-retinol by RDHs, including RDH8. The fraction of all-*trans*-retinal that dissociates into disc lumens is transported by ABCA4 into the cytoplasm (4) before it is reduced. Thus, condensation products can be generated both within the disc lumens and the cytoplasm. Loss of ABCA4 and RDH8 exacerbates this condensation, which is reminiscent of an accelerated aging process.

mechanism-based pharmacological agents to prevent progressive retinal degeneration by aberrant reactions of the visual cycle.

MATERIALS AND METHODS

Animals—*Rdh8*$^{-/-}$ mice were generated and genotyped as previously described (16). *Abca4*$^{-/-}$ mice also were generated by standard procedures (Ingenious Targeting, Inc., Stony Brook, NY). The targeting vector was constructed by replacing exon 1 with the neo cassette as described by Weng *et al.* (13). No immunoreactivity against ABCA4 was detected in eye extracts from these mice by immunocytochemistry or immunoblotting. *Abca4*$^{-/-}$ mice were maintained with either pigmented 129Sv/Ev or C57BL/6 mixed backgrounds, and their siblings were used for most experiments. *Rdh8*$^{-/-}$*Abca4*$^{-/-}$ mice were established by cross-breeding *Abca4*$^{-/-}$ mice with *Rdh8*$^{-/-}$ mice. Genotyping of mice was carried out by PCR with primers ABCR1 (5′-gcccagtggtcgatctgtctagc-3′) and ABCR2 (5′-cggacacaaaggccgctaggaccacg-3′) for wild type (WT) (619 bp) and A0 (5′-ccacagcacacatcagcatttctcc-3′) and N1 (5′-tgcgaggccagaggccacttgtgtagc-3′) for targeted deletion (455 bp). PCR products were cloned and sequenced to verify their identities. *Rdh8*$^{-/-}$*Abca4*$^{-/-}$ mice were fertile and showed no obvious developmental abnormalities.

All mice used in this study were housed in the animal facility at the School of Medicine, Case Western Reserve University, where they were maintained either under complete darkness or in a 12-h light (less than 10 lux)/12-h dark cycle environment. For acute light exposure, mice were dark-adapted for 24 h and then exposed to fluorescent light at 10,000 lux for 60 min. Retinal damage was analyzed 7 days after this light exposure. All other manipulations were done under dim red light transmitted through a Kodak No. 1 Safelight filter (transmittance >560 nm). All animal procedures and experiments were approved by the Case Western Reserve University Animal Care Committees and conformed to both the recommendations of the American Veterinary Medical Association Panel on Euthanasia and the Association of Research for Vision and Ophthalmology.

Synthesis and Analyses of RALdi—RALdi was extracted from six mouse eyes by homogenization with 3 ml of hexane/ethyl acetate (66%:33%) and use of a glass/glass homogenizer. After evaporation of solvent, dried extracts were dissolved in 150 μl of acetonitrile with 0.1% trifluoroacetic acid and passed through a Teflon syringe filter (National Scientific Co., Rockwood, TN). Samples (100 μl) were loaded on C18 columns (Phenomenex, Torrance, CA) and analyzed with a gradient of isopropyl alcohol in acetonitrile (0–25%) containing 0.1% formic acid for 20 min at a flow rate of 1 ml/min. Molecular masses and fragmentation patterns of an authentic standard synthesized by a published method (17) and RALdi extracted from mouse eyes were confirmed by liquid chromatography/mass spectrometry under chromatographic conditions described above with an LXQ mass spectrometer (Thermo Scientific, Waltham, MA) equipped with an APCI source and combined with a 1100 series HPLC (Agilent Technologies, Santa Clara, CA).

Retinylamine Treatment—Retinylamine was synthesized and administered by oral gavage as previously described (18).

Electroretinogram (ERG)—All ERG procedures were performed by published methods (16).

Histology and Immunocytochemistry—The histological and immunocytochemical procedures employed were previously described (16).

Retinoid and A2E Analyses—Experimental procedures related to extraction, derivatization, and separation of retinoids from dissected mouse eyes were carried out as previously described (16). Quantification of A2E by HPLC was performed by comparison with known concentrations of pure synthetic A2E (15).

Angiography—Angiograms were performed after a 400-μl intracardiac injection of 10 mg/ml fluorescein isothiocyanate-conjugated high molecular weight dextran (FD-2000S; Sigma) into anesthetized mice (19).

VEGF Quantification—Mouse eyes were enucleated and submerged immediately in ice-cold phosphate-buffered saline. Cornea, lens, and outside connective tissues were carefully removed, and eyes were placed in 500 μl of lysis buffer containing 10 mM NaF, 300 mM NaCl, 50 mM Tris, pH 7.4, 1% Triton X-100, 10% glycerol, and 1 mM EDTA with a 1% volume (5 μl) of phosphatase and protease inhibitor mixture (Sigma). Samples were sonicated and stored at −80 °C. After two freeze-thaw cycles, they were centrifuged at 14,000 rpm for 10 min at 4 °C. Levels of VEGF in the supernatant were determined with a mouse enzyme-linked immunosorbent assay kit (R&D Systems, Minneapolis, MN) according to the manufacturer's instructions. Protein concentrations in the supernatants were measured by the Bradford method (Bio-Rad).

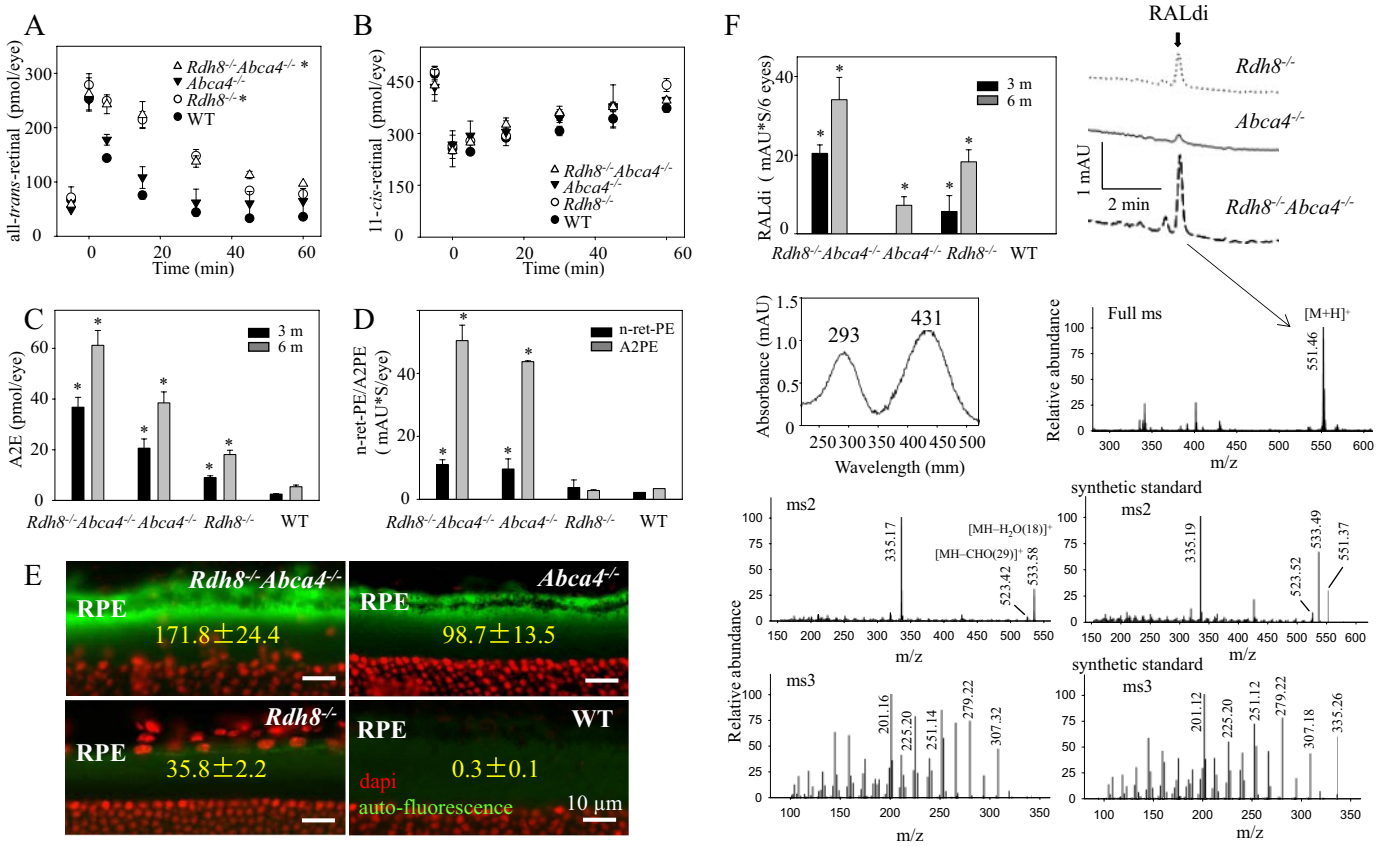

FIGURE 1. **Reactions of the visual cycle and all-*trans*-retinal condensation in WT, *Rdh8*$^{-/-}$*Abca4*$^{-/-}$, *Rdh8*$^{-/-}$, and *Abca4*$^{-/-}$ mice.** *A*, kinetics of all-*trans*-retinal reduction after a flash that bleached ~40% of visual pigment. *B*, 11-*cis*-retinal formation in *Rdh8*$^{-/-}$, *Abca4*$^{-/-}$, and *Rdh8*$^{-/-}$*Abca4*$^{-/-}$ mice at the age of 6 weeks. Retinoids were quantified by HPLC in samples collected at different time points after the flash. *Bars*, S.E. ($n > 3$; *, $p < 0.01$) *versus* WT animals. *C*, A2E amounts in the eyes of *Rdh8*$^{-/-}$, *Abca4*$^{-/-}$, and *Rdh8*$^{-/-}$*Abca4*$^{-/-}$ mice at 3 and 6 months of age were quantified by HPLC. *Bars*, S.E. ($n > 6$; *, $p < 0.01$) *versus* WT animals. *D*, quantification of retinal *N*-retinylidene-phosphatidylethanolamine (*n-ret-PE*) and A2PE (intermediates in A2E formation) was performed in *Rdh8*$^{-/-}$, *Abca4*$^{-/-}$, and *Rdh8*$^{-/-}$*Abca4*$^{-/-}$ mice at the ages of 3 and 6 months. Mice were reared under 12-h light (less than 10 lux)/12-h dark conditions. *Bars*, S.E. ($n > 6$; *, $p < 0.01$) *versus* WT animals. *E*, retinal autofluorescence levels (*green*) and nuclear staining (*red*; DAPI) at 6 months of age were detected with a fluorescent microscope. The *numbers* indicate fluorescence intensity (arbitrary units) calculated with Image J. *Bar*, 10 μm. *F*, detection of RALdi. *Top left*, amounts of RALdi in six eyes of 3- and 6-month-old animals. The *numbers* indicate areas (milli-absorption units (*mAU*S*)) of RALdi peaks. *Bars*, S.E. (more than 18 eyes were used for each group; *, $p < 0.01$) *versus* WT animals. *Top right*, HPLC chromatograms of RALdi in six eyes of 6-month-old animals. The *numbers* indicate areas (milli-absorption units (*mAU*S*)) of RALdi peaks. *Middle left*, UV-visible spectrum of RALdi peak fraction isolated from the retinas of 6-month-old *Rdh8*$^{-/-}$*Abca4*$^{-/-}$ mice. *Middle right*, full MS spectra of RALdi from retinas of 6-month-old *Rdh8*$^{-/-}$*Abca4*$^{-/-}$ mice. *Bottom*, MS spectra of RALdi from retinas of 6-month-old *Rdh8*$^{-/-}$*Abca4*$^{-/-}$ mice (*left*) and a synthetic standard (*right*). RALdi has a mass of 550.86.

Statistical Analyses—Data representing the means ± S.E. for the results of at least three independent experiments were compared by the one-way analysis of variance test.

RESULTS

All-trans-retinal Clearance and A2E Production—Because ABCA4 and RDH8 are responsible for all-*trans*-retinal metabolism in ROS/COS (1), rates of all-*trans*-retinal clearance and 11-*cis*-retinal production were examined in 6-week-old *Rdh8*$^{-/-}$, *Abca4*$^{-/-}$, and *Rdh8*$^{-/-}$*Abca4*$^{-/-}$ mice after an intense light flash that bleached ~40% of the total amount of rhodopsin. Both *Rdh8*$^{-/-}$ and *Rdh8*$^{-/-}$*Abca4*$^{-/-}$ mice showed a delayed clearance of all-*trans*-retinal, whereas rates of all-*trans*-retinal clearance in *Abca4*$^{-/-}$ mice were comparable with those of WT mice (Fig. 1*A*). No significant differences were observed in the rates of 11-*cis*-retinal regeneration among these animals (Fig. 1*B*). Attenuated rates of all-*trans*-retinal clearance, such as found in *Rdh8*$^{-/-}$ and *Rdh8*$^{-/-}$*Abca4*$^{-/-}$ mice, could lead to all-*trans*-retinal condensation. A2E and RALdi, condensation products of all-*trans*-retinal, are formed by hydrolysis of phosphate esters of either A2PE or RALdi-PE, phosphatidyl bisretinoid precursors generated by ROS and COS when all-*trans*-retinal, released from photoactivated visual pigments (2), conjugates with phosphatidylethanolamine instead of undergoing reduction to all-*trans*-retinol. Therefore, we determined A2E levels in mouse eyes as a surrogate product of these condensation reactions. Six-month-old *Rdh8*$^{-/-}$*Abca4*$^{-/-}$ mice had the highest amounts of A2E compared with single knock-out animals, but surprisingly, 3–6-month-old *Abca4*$^{-/-}$ mice accumulated more A2E than *Rdh8*$^{-/-}$ mice (Fig. 1*C*), although *Abca4*$^{-/-}$ mice cleared all-*trans*-retinal more rapidly (Fig. 1*A*). A similar accumulation relationship (*i.e.* *Rdh8*$^{-/-}$*Abca4*$^{-/-}$ highest, *Abca4*$^{-/-}$ next, and *Rdh8*$^{-/-}$ least) was found for the intermediates in A2E formation, *N*-retinylidene-phosphatidylethanolamine, and A2PE (Fig. 1*D*). Localization of accumulated fluorophores was demonstrated by fluorescence analysis of retinal sections (Fig. 1*E*). As expected, we detected the highest level of fluorescence in the RPE from *Rdh8*$^{-/-}$*Abca4*$^{-/-}$ mice followed in order by RPE samples from *Abca4*$^{-/-}$ and *Rdh8*$^{-/-}$ mice. Recently, RALdi

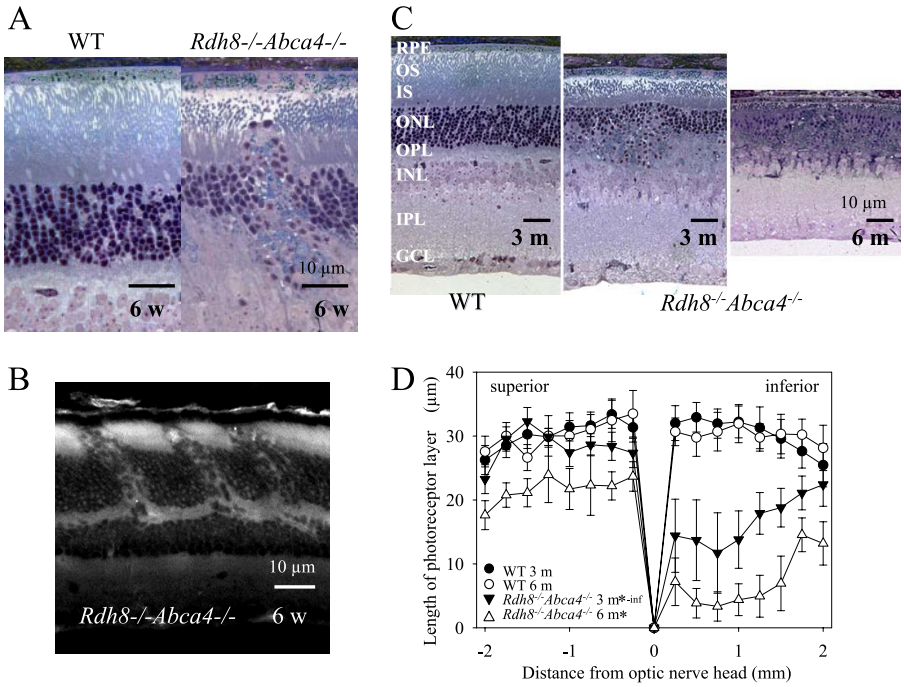

FIGURE 2. **Retinal histology in *Rdh8*$^{-/-}$*Abca4*$^{-/-}$ mice.** *A*, retinal rosette formation is apparent in 6-week-old *Rdh8*$^{-/-}$*Abca4*$^{-/-}$ mice. *Bars*, 10 μm. *B*, a representative image is shown ($n > 10$) of local changes corresponding to an area supported by a single RPE cell in 6-week-old *Rdh8*$^{-/-}$*Abca4*$^{-/-}$ mice. *Bar*, 10 μm. Rosette formation was observed in all such mice. *C*, morphology of WT and *Rdh8*$^{-/-}$*Abca4*$^{-/-}$ retinas from 3- and 6-month-old mice kept under room light (less than 10 lux). Progressive reduction of photoreceptor and loss of outer nuclear layers compared with WT retina were evidenced by retinas from *Rdh8*$^{-/-}$*Abca4*$^{-/-}$ mice. *OS*, outer segment; *IS*, inner segment; *ONL*, outer nuclear layer; *OPL*, outer plexiform layer; *INL*, inner nuclear layer; IPL, inner plexiform layer. *Bars*, 10 μm. *D*, photoreceptor thickness plotted for WT and *Rdh8*$^{-/-}$*Abca4*$^{-/-}$ mice at 3 and 6 months of age. *Rdh8*$^{-/-}$*Abca4*$^{-/-}$ mice showed decreased photoreceptor thickness, especially in the inferior retina. *Bars*, S.E. ($n > 6$; *, $p < 0.01$) *versus* WT animals.

was shown to exhibit even greater cytotoxicity than A2E (20). We found more RALdi in *Rdh8*$^{-/-}$ than in *Abca4*$^{-/-}$ mice but detected the highest amount in *Rdh8*$^{-/-}$*Abca4*$^{-/-}$ mice (Fig. 1*F*). This result suggests that a delayed clearance of all-*trans*-retinal, most likely from ROS cytoplasm, is critical to RALdi formation. Retinoic acids were not detected in *Rdh8*$^{-/-}$*Abca4*$^{-/-}$ eyes before or after light exposure (data not shown).

Retinal Degeneration in Rdh8$^{-/-}$*Abca4*$^{-/-}$ *Mice*—Three-week-old *Rdh8*$^{-/-}$*Abca4*$^{-/-}$ mice did not display any retinal dystrophy, but dramatic regional retinal degeneration was evident by 4–6 weeks of age (Fig. 2, *A* and *B*). By 3 months of age, retinal changes were advanced as manifested by reduced thickness of the photoreceptor layer, fewer and more scattered photoreceptor nuclei (Fig. 2*C*), and formation of retinal rosettes by 6 weeks of age (Fig. 2*A*). Further progression of retinal degeneration was detected at 6 months of age (Fig. 2, *C* and *D*). Cone photoreceptor atrophy, first noted in 4–6-week-old mice, gradually increased with age (Fig. 3, *A* and *B*). Cone and rod degeneration was more severe in the inferior central area than in the superior area (Fig. 3*C*). 11-*cis*-Retinal, which quantitatively reflects the level of rhodopsin, decreased with age in *Rdh8*$^{-/-}$*Abca4*$^{-/-}$ mice (Fig. 3*C*). Retinal abnormalities were not detected in age-matched *Rdh8*$^{-/-}$ or *Abca4*$^{-/-}$ mice (Fig. 3*A*) nor were they found in 3-month-old *Rdh8*$^{-/-}$*Abca4*$^{-/-}$ mice kept in the dark (data not shown). Retinal degeneration in *Rdh8*$^{-/-}$*Abca4*$^{-/-}$ mice was accompanied by complement deposition (Fig. 3*D*). ERGs obtained to assess retinal function showed that amplitudes of a- and b-waves under scotopic conditions were significantly attenuated in 3-month-old *Rdh8*$^{-/-}$*Abca4*$^{-/-}$ mice (Fig. 3*E*, *left*) that also displayed reduced flicker ERG responses at 20 and 30 Hz (Fig. 3*E*, *right*). These data clearly indicate cone/rod dystrophy in *Rdh8*$^{-/-}$*Abca4*$^{-/-}$ mice. Severely delayed dark adaptation rates similar to those found in *Rdh8*$^{-/-}$ mice also were observed in *Rdh8*$^{-/-}$*Abca4*$^{-/-}$ mice of the same age (data not shown). The incidence of retinal degeneration in the different knock-out mice is summarized in Fig. 3*F*. Mice carry two different alleles of *Rpe65* that have amino acid variations at position 450 (21), with the Leu variant known to accumulate more A2E than the Met variant (22). Interestingly, *Rdh8*$^{-/-}$*Abca4*$^{-/-}$ 3-month-old mice with the Met variation showed a 43.8% incidence of retinal degeneration, whereas identically aged *Rdh8*$^{-/-}$*Abca4*$^{-/-}$ mice with Leu exhibited a 97.5% incidence. These rates of retinal degeneration incidence were well correlated with the amounts of A2E found (Met *versus* Leu; 21.4 ± 2.7 *versus* 38.8 ± 3.9 pmol/eye at 3 months of age). Therefore, the incidence of retinal degeneration correlates well with the higher visual cycle rates found in mice that carried the Leu^{450} variant of *Rpe65*.

Ultrastructure of Degenerated RPE in Rdh8$^{-/-}$*Abca4*$^{-/-}$ *Mice*—The RPE of affected 3-month-old *Rdh8*$^{-/-}$*Abca4*$^{-/-}$ mice revealed increased thickness with more pigmented granules as compared with the RPE of WT mice (Fig. 4, *A–D*). We also observed changes in the Bruch's membrane of these double knock-out mice (Fig. 4, *E* and *F*). Interestingly, the RPE of *Rdh8*$^{-/-}$*Abca4*$^{-/-}$ mice exhibited accumulation of lipofuscin, lipid granules, and vacuolarization (Fig. 4*G*). Some cells in the RPE had died, and their remnants were more obvious in the inferior area of the retina near the optic nerve head (Fig. 4*H*). Dead cells in the RPE contained undigested ROS/COS and basal laminar deposits that invaded Bruch's membrane (Fig. 4*I*). Lipofuscin accumulation and vacuolarization around lipofuscin in the RPE also was detected by electron microscopy of these mice at 3 months of age (Fig. 4*J*), indicating the toxicity of A2E as a cationic detergent (23). Lipofuscin deposits occurred between the RPE and the ROS (Fig. 4*K*), and drusen deposits were detected under the RPE (Fig. 4*L*). These findings correspond with abnormalities found in the retinas of humans with age-related macular degeneration (AMD), a leading cause of blindness in developed counties (24, 25).

Choroidal Neovascularization and Levels of VEGF—Choroidal neovascularization, a hallmark of wet type AMD, was visu-

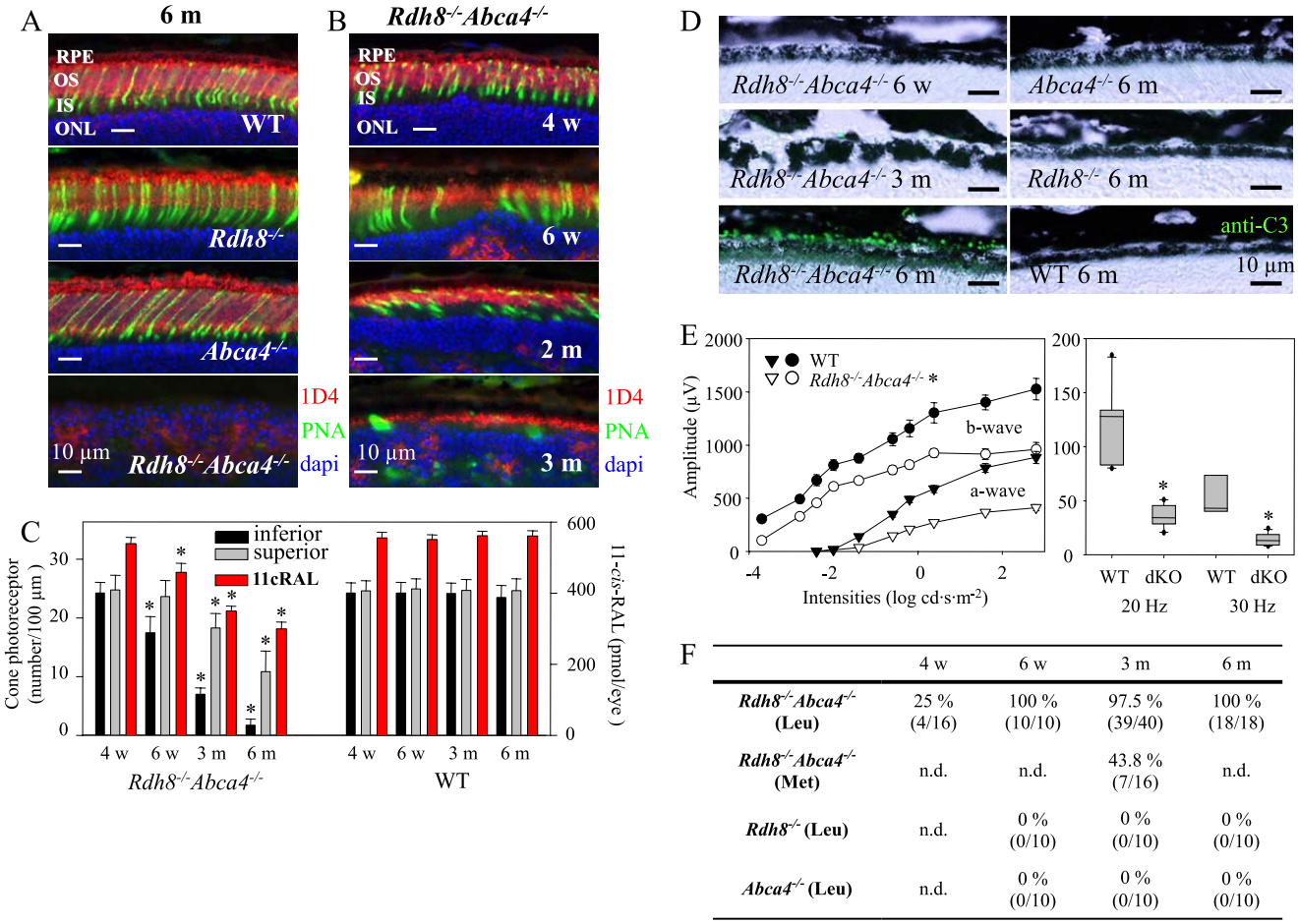

F

	4 w	6 w	3 m	6 m
***Rdh8*$^{-/-}$*Abca4*$^{-/-}$ (Leu)**	25 % (4/16)	100 % (10/10)	97.5 % (39/40)	100 % (18/18)
***Rdh8*$^{-/-}$*Abca4*$^{-/-}$ (Met)**	n.d.	n.d.	43.8 % (7/16)	n.d.
***Rdh8*$^{-/-}$ (Leu)**	n.d.	0 % (0/10)	0 % (0/10)	0 % (0/10)
***Abca4*$^{-/-}$ (Leu)**	n.d.	0 % (0/10)	0 % (0/10)	0 % (0/10)

FIGURE 3. ***Rdh8*$^{-/-}$*Abca4*$^{-/-}$ mice develop cone-rod dystrophy.** *A*, retinal structures of *Rdh8*$^{-/-}$, *Abca4*$^{-/-}$, and *Rdh8*$^{-/-}$*Abca4*$^{-/-}$ 6-month-old mice (inferior retina) are shown with cone photoreceptor (*green*, PNA), outer segment (*red*, anti-rhodopsin 1D4), and nuclear staining (*blue*, DAPI). Severe cone-rod dystrophy is apparent only in *Rdh8*$^{-/-}$*Abca4*$^{-/-}$ mice. *OS*, outer segment; *IS*, inner segment; *ONL*, outer nuclear layer. *Bars*, 10 μm. *B*, retinal structure was assessed in *Rdh8*$^{-/-}$*Abca4*$^{-/-}$ mice at 4 weeks, 6 weeks, 2 months, and 3 months of age with cone photoreceptor (*green*, PNA), outer segment (*red*, anti-rhodopsin 1D4), and nuclear staining (*blue*, DAPI). Progressive retinal dystrophy was detected by 6 weeks of age. *OS*, outer segment; *IS*, inner segment. *Bars*, 10 μm. *C*, populations of cone photoreceptors and 11-*cis*-retinal levels in *Rdh8*$^{-/-}$*Abca4*$^{-/-}$ and WT retinas. Cones were examined by counting PNA-stained cone photoreceptors, and 11-*cis*-retinal was quantified by HPLC. Numbers of cone photoreceptors/100 μm in areas of the inferior and superior central retina located 500 μm from the optic nerve head in mice at 4 weeks, 6 weeks, 3 months, and 6 months of age are indicated. Retinoids were extracted from 48-h dark-adapted mice. *Bars*, S.E. ($n > 6$; *, $p < 0.01$) *versus* WT animals. *D*, complement deposition was examined with anti-C3 antibody (*green*, C3 (H300) antibody; Santa Cruz Biotechnology, Inc. (Santa Cruz, CA)) in *Rdh8*$^{-/-}$*Abca4*$^{-/-}$ mice at 6 weeks, 3 months, and 6 months of age. Inferior retinas are presented. The C3 signal was detected in Bruch's membrane of 6-month-old *Rdh8*$^{-/-}$*Abca4*$^{-/-}$ mice, and a weak signal also was observed in these mice at 3 months of age. Representative images are shown ($n > 6$). Complement deposition was noted in all 6-month-old *Rdh8*$^{-/-}$*Abca4*$^{-/-}$ mice. *E*, full-field ERG responses of *Rdh8*$^{-/-}$*Abca4*$^{-/-}$ mice at 3 months of age. *Left*, ERG responses recorded under scotopic conditions. Both a- and b-wave amplitudes plotted as a function of light intensity were significantly attenuated in 3-month-old *Rdh8*$^{-/-}$*Abca4*$^{-/-}$ mice compared with the same age WT animals. *Bars*, S.E. ($n = 6$; *, $p < 0.01$). *Right*, flicker ERGs recorded at 20 and 30 Hz showed marked decreases in *Rdh8*$^{-/-}$*Abca4*$^{-/-}$ (*dko*) mice. The *boxes* indicate S.D., and *bars* indicate maximum and minimum values of results ($n > 6$; *, $p < 0.01$). *F*, effect of variations in the *Rpe65* gene on the incidence of retinal changes. Two variants of the *Rpe65* gene at position 450 (Leu or Met) were investigated. The Leu variant showed more retinopathy at 3 months than the Met variant. Numbers of eyes tested are presented. *n.d.*, not determined.

alized by fluorescent angiography (19). The surface vasculature of *Rdh8*$^{-/-}$*Abca4*$^{-/-}$ retinas from 10-month-old mice was well preserved (Fig. 5*A*). No abnormal vascularization was detected in WT RPE (Fig. 5*B*), whereas aberrant growth of choroidal neovascularization was seen in the RPE of 10-month-old *Rdh8*$^{-/-}$*Abca4*$^{-/-}$ mice (Fig. 5*C*). We also detected choroidal neovascularization in 22.2% ($n = 18$) of 6-month-old *Rdh8*$^{-/-}$*Abca4*$^{-/-}$ mice, a percentage that increased to 37.5 ($n = 8$) in 10-month-old double knock-out animals. Retinal blood circulation was maintained in the upper layers of the retina (ONL to GCL) in 10-month-old WT mice (Fig. 5*D*), but penetration of neovascularizations from the choroid into the RPE and photoreceptors was noted in identically aged *Rdh8*$^{-/-}$*Abca4*$^{-/-}$ mice (Fig. 5, *E* and *F*). Immunostaining for CD31 (an endothelial cell marker) also demonstrated choroidal neovascularization growth (Fig. 5*G*). Hyperpigmentation and irregular pigment distribution were seen in the retinas of 6-month-old *Rdh8*$^{-/-}$*Abca4*$^{-/-}$ mice, suggesting that irregular pigmentation may correlate with choroidal neovascularization growth (data not shown). These findings were accompanied by age-related increasing levels of VEGF in the eye detected in 6- and 12-month-old mice by specific enzyme-linked immunosorbent assay (Fig. 5*H*).

Light Exposure-induced Retinal Degeneration—Light exposure is critical for A2E accumulation and induction of related toxicity (26). To determine if the retinal degeneration in *Rdh8*$^{-/-}$*Abca4*$^{-/-}$ mice is influenced by light, we exposed 4-week-old *Abca4*$^{-/-}$, *Rdh8*$^{-/-}$, and *Rdh8*$^{-/-}$*Abca4*$^{-/-}$ mice

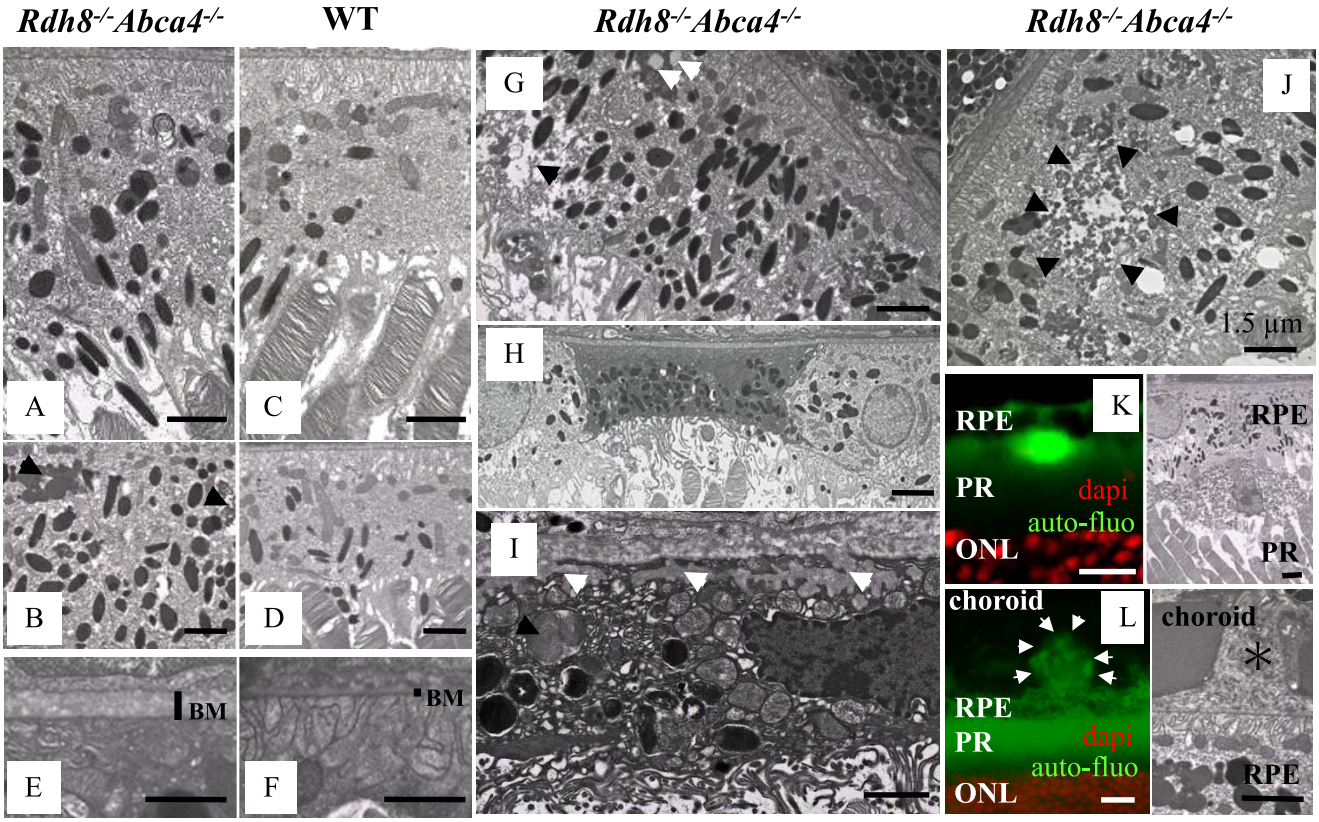

FIGURE 4. **Electron micrographic analyses of *Rdh8*$^{-/-}$*Abca4*$^{-/-}$ mice.** *A* and *B*, electron micrographs of the RPE in 3-month-old *Rdh8*$^{-/-}$*Abca4*$^{-/-}$ mice kept under room light (<10 lux). Swollen RPE with increased pigmented bodies and lipofuscin accumulation (*black arrows*) are shown. *C* and *D*, electron micrographs of healthy RPE in WT 3-month-old mice. *E* and *F*, Bruch's membrane (*BM*) of 3-month-old *Rdh8*$^{-/-}$*Abca4*$^{-/-}$ mice exhibits increased thickness as compared with WT. *G*, the RPE of 3-month-old *Rdh8*$^{-/-}$*Abca4*$^{-/-}$ mice reveals lipid inclusions (*white arrows*) and vacuolarization (*black arrow*). *H*, RPE death evidenced by nuclear ablation and changes in mitochondrial membranes of *Rdh8*$^{-/-}$*Abca4*$^{-/-}$ mice. *I*, basal laminar deposits (*white arrows*) found in the dead RPE; these deposits invade Bruch's membrane and form drusen. Undigested outer segments (*black arrow*) also are shown. *J*, electron microscopic image shows lipofuscin accumulation (*black arrows*) in the RPE of 3-month-old *Rdh8*$^{-/-}$*Abca4*$^{-/-}$ mice. *K* (*left*), a lipofuscin deposit is seen between the RPE and the ROS of these mice. *Right*, the lipofuscin deposit corresponding to that shown in the left panel is imaged by electron microscopy. *L* (*left*), drusen formation (*white arrows*) is seen under the RPE. *Right*, electron microscopic image of drusen (*) corresponding to that in the *left panel* is pictured. *Bars*, 1.5 μm. Representative images are shown. Similar findings were detected in all six eyes analyzed.

without such degeneration to 10,000 lux of fluorescent light for 60 min. As shown in Fig. 6, retinal degeneration with retinal folds was induced by this light in all genotypes. Retinal degeneration was most severe in *Rdh8*$^{-/-}$*Abca4*$^{-/-}$ mice with changes similar to those typical of $NaIO_3$-induced RPE death (Fig. S1) (27). Mild retinal changes also were induced by this light in all examined 3-month-old *Rdh8*$^{-/-}$ mice, indicating that accumulation of all-*trans*-retinal during light exposure also promoted retinal changes. Fifteen-month-old *Abca4*$^{-/-}$ mice failed to exhibit retinal degeneration under regular light conditions (28), but 10,000-lux fluorescent light exposure did induce mild retinal degeneration in 41.7% ($n = 12$) of 3-month-old *Abca4*$^{-/-}$ mice. WT mice did not show any retinal changes under these conditions. Pretreatment with retinylamine, a long lasting retinoid cycle inhibitor (18, 29, 30), ameliorated the severe retinal degeneration observed in 4-week-old *Rdh8*$^{-/-}$*Abca4*$^{-/-}$ mice. This observation led us to document the effects of retinylamine treatment more extensively.

Retinylamine-attenuated A2E Production and Retinal Degeneration—Retinylamine acts on the retinoid cycle by inhibiting 11-*cis*-retinal production (18, 29, 31). By slowing regeneration of visual pigments, in turn, production of all-*trans*-retinal caused by bleaching of these receptors is attenuated (1). To determine if reduced accumulation of condensation products protects against retinal degeneration, we treated *Rdh8*$^{-/-}$*Abca4*$^{-/-}$ mice with retinylamine. Treatment with 1 mg of retinylamine by oral gavage was given to 1-month-old mice either once every week or every other week for 3 months. These treatment regimens were chosen, because retinylamine is amidated and stored, providing long lasting efficacy after a single dose (18, 29, 30). This dose suppressed 11-*cis*-retinal regeneration up to 1 week in WT mice (30). Under 12-h light/12-h dark conditions, mice undergoing either treatment regimen exhibited reduced A2E levels to near those found in animals kept in darkness (Fig. 7*A*). Degeneration was not detected anywhere in the retinas of retinylamine-treated mice, whereas vehicle-treated animals developed severe pathology in the inferior cone-rich retina (Fig. 7, *B* and *C*). Because 1 mg of retinylamine given every 2 weeks by gavage was effective in preventing marked A2E accumulation and retinal damage, we tested the effects of administering the alternate week regimen to *Rdh8*$^{-/-}$*Abca4*$^{-/-}$ mice over different time periods. As expected, 7-month-old *Rdh8*$^{-/-}$*Abca4*$^{-/-}$ mice treated with only vehicle for 6 months showed severe retinal degeneration with the greatest A2E accumulation (Fig. 7, *D* and *E*). *Rdh8*$^{-/-}$

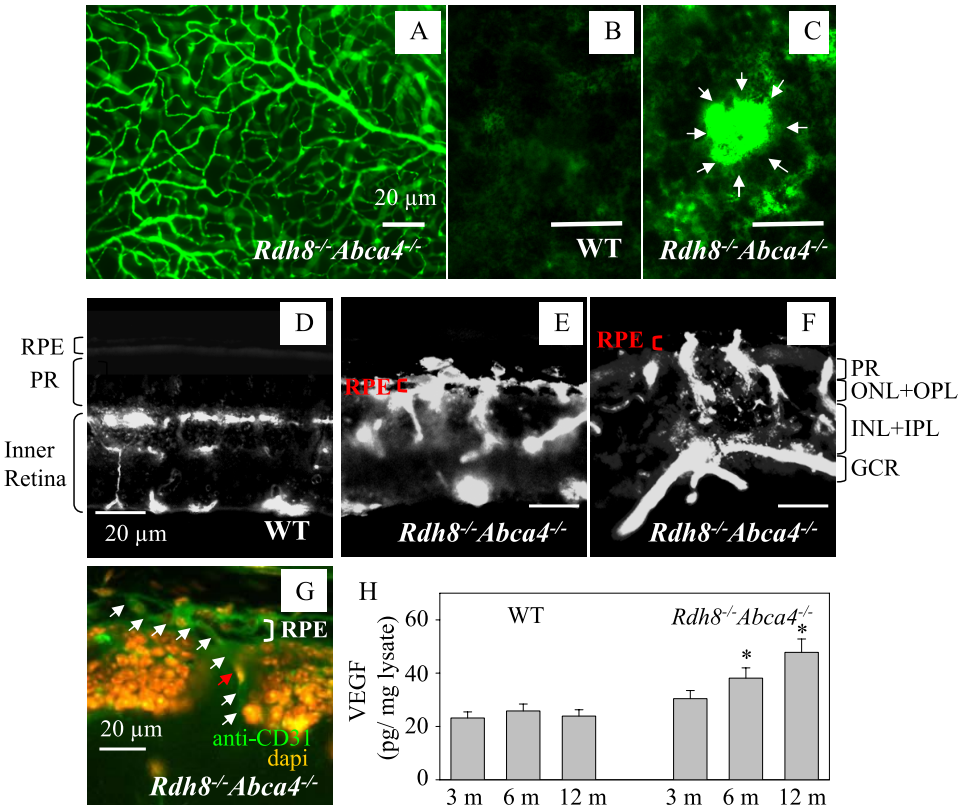

FIGURE 5. **Choroidal neovascularization in 10-month-old *Rdh8*$^{-/-}$*Abca4*$^{-/-}$ mice.** *A*, retinal vasculature of a 10-month-old *Rdh8*$^{-/-}$*Abca4*$^{-/-}$ mouse is shown. A similar image was obtained from WT mice of comparable age (not shown). Mice were kept under room light (less than 10 lux). *B*, blood vessels in the RPE layer of 10-month-old WT mice. *C*, blood vessels in the RPE layer of 10-month-old *Rdh8*$^{-/-}$*Abca4*$^{-/-}$ mice. *White arrows*, choroidal neovascularization. *D*, angiograph of a retina from a 10-month-old WT mouse is shown. *PR*, photoreceptor. *E*, choroidal neovascularization growth in the central area of the inferior retina of a 10-month-old *Rdh8*$^{-/-}$*Abca4*$^{-/-}$ mouse with severely impaired photoreceptors. *F*, choroidal neovascularization growth in the peripheral retinal area of a 10-month-old *Rdh8*$^{-/-}$*Abca4*$^{-/-}$ mouse showing less impairment of photoreceptors (compared with the central area). *PR*, photoreceptor; *ONL*, outer nuclear layer; *OPL*, outer plexiform layer; *INL*, inner nuclear layer; *IPL*, inner plexiform layer; *GCL*, ganglion cell layer. *Bars*, 20 μm. *G*, choroidal neovascularization growths from choroid into the RPE and ROS in retina from a 10-month-old *Rdh8*$^{-/-}$*Abca4*$^{-/-}$ mouse. This slide was stained with an anti-endothelial cell marker antibody (anti-CD31 antibody; *green*) and an antinuclear antibody (DAPI; *orange*). The *white arrows* show choroidal neovascularization, and the *red arrow* indicates nuclei of the choroidal neovascularization endothelium. *Bar*, 20 μm. *H*, amounts of VEGF in the eye were analyzed by a specific enzyme-linked immunosorbent assay. Increasing levels of VEGF were detected in 6- and 12-month-old *Rdh8*$^{-/-}$*Abca4*$^{-/-}$ as compared with WT mice. *Bars*, S.E. ($n > 3$; *, $p < 0.01$) *versus* WT animals.

DISCUSSION

Herein, we describe a retinopathy in mice induced by disrupted all-*trans*-retinal clearance. Double knock-out mice lacking ABCA4 and RDH8 manifested retinal abnormalities with hallmark features that include A2E/RALdi/lipofuscin accumulation, RPE/photoreceptor atrophy, drusen, basal laminar deposits, thickened Bruch's membrane, and choroidal neovascularization. Most of these changes were evident in the first 2–3 months of life and were exacerbated by exposure to bright light. Mice lacking either ABCA4 or RDH8 alone failed to show much retinal pathology despite accumulation of A2E (*Abca4*$^{-/-}$ mice) (13) or delayed clearance of all-*trans*-retinal (*Rdh8*$^{-/-}$ mice) (16).

Accumulation of All-trans-retinal Condensation Products in the RPE—A2E accumulation in the RPE was greater in mice lacking the *Abca4* gene than in those without the *Rdh8* gene. The reason for this difference could be that residual all-*trans*-retinal remains in the disc lumen longer than in the cytoplasm of *Abca4*$^{-/-}$ mice, thereby allowing condensation to take place before ROS/COS are phagocytized by the RPE, which are completely renewed every week or so. Thus, all-*trans*-retinal condensation reactions in *Abca4*$^{-/-}$ mice would not be linked to the clearance of all-*trans*-retinal that occurs within 1 h after intense bleach. Recently, RALdi was shown to be more toxic to the RPE than A2E (20). Accumulation of all-*trans*-retinal leads to formation of RALdi in *Rdh8*$^{-/-}$ mice and results directly from impaired clearance of all-*trans*-retinal in the cytoplasm of ROS or COS. Indeed, more RALdi was detected in RDH8-deficient mice than in *Abca4*$^{-/-}$ mice (Fig. 1*F*), together with a higher incidence of light-induced retinal changes (100% in *Rdh8*$^{-/-}$ *versus* 41.7% in *Abca4*$^{-/-}$ mice) (Fig. 6). Greater accumulation of all-*trans*-retinal and RALdi in *Rdh8*$^{-/-}$ mice implies an important role of these reactive molecules in retinal degeneration. Significantly, *Rdh8*$^{-/-}$*Abca4*$^{-/-}$ mice accumulated substantially more A2E and RALdi than all of the other tested mutant mice (Fig. 1, *C* and *F*).

Retinals and Degeneration of the Retina—Although retinals are essential to vision because of their ability to regenerate visual chromophores, they also are chemically reactive and toxic, so cells have developed specific mechanisms to protect against

Abca4$^{-/-}$ mice gavaged at an early age (1 month of age treated for 3 months) showed amounts of A2E similar to those of older mice gavaged for the same period (4 months of age treated for 3 months). A2E levels in both of these groups were significantly reduced as compared with vehicle-treated controls, but they also were higher than levels found in dark-adapted animals. Levels of A2E in young 1-month-old *Rdh8*$^{-/-}$*Abca4*$^{-/-}$ mice treated for 6 months were only marginally increased as compared with those found in dark-reared mice, and retinal histology showed minimal changes in only 50% of these treated animals. However, untreated 7-month-old dark-reared *Rdh8*$^{-/-}$*Abca4*$^{-/-}$ mice did have increased amounts of A2E as compared with same age (7 months) WT animals raised under regular 12-h light/12-h dark conditions (*Rdh8*$^{-/-}$*Abca4*$^{-/-}$ *versus* WT; 17.5 ± 2.0 *versus* 5.4 ± 0.7 pmol/eye of A2E). Only minimal retinal changes were observed in 67% of these dark-reared *Rdh8*$^{-/-}$*Abca4*$^{-/-}$ mice (Fig. 7, *D* and *E*; WT not shown).

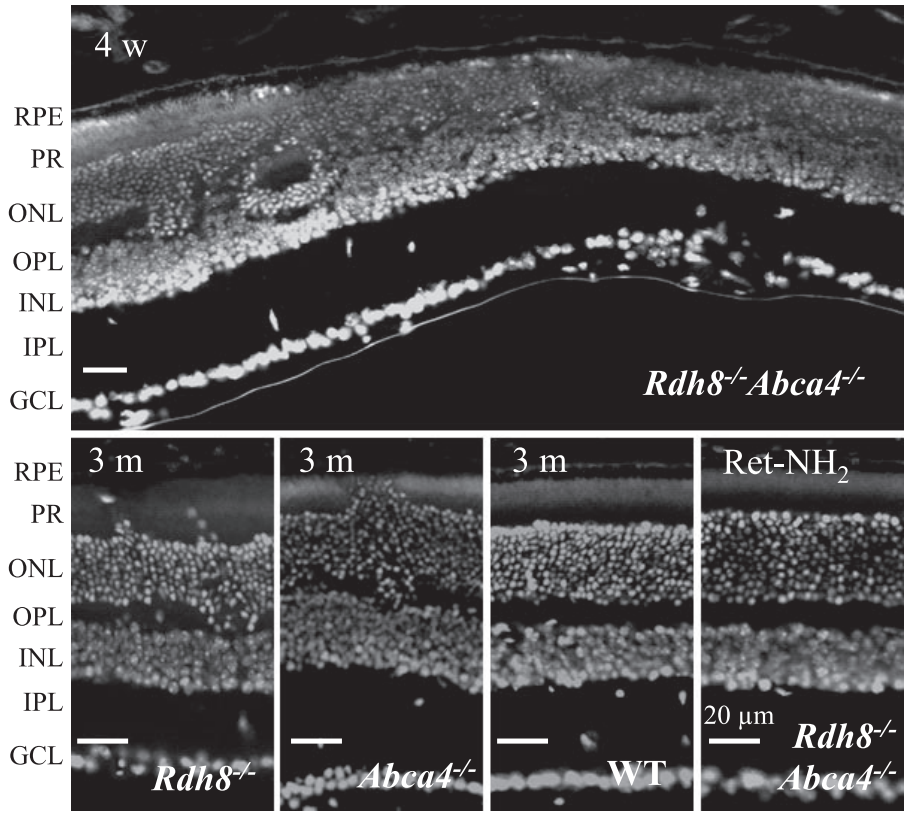

FIGURE 6. **Light exposure accelerates retinal degeneration.** Light exposure (10,000 lux for 60 min) accelerated retinal degeneration in *Rdh8*$^{-/-}$*Abca4*$^{-/-}$ mice as seen by DAPI nuclear staining. Prior to examination, mice were maintained in the dark for 7 days after light exposure. *Top*, inferior retina of a light-exposed 4-week-old *Rdh8*$^{-/-}$*Abca4*$^{-/-}$ mouse shows widely distributed pathology, including severe photoreceptor loss with rosette formation. *Bottom*, mild changes occurred in light-exposed retinas from 3-month-old *Rdh8*$^{-/-}$ and *Abca4*$^{-/-}$ mice as compared with normal retina from light-exposed 3-month-old WT mice. Retinylamine (*Ret-NH$_2$*) treatment (1-mg gavage 6 h prior to the light exposure) prevented the severe degeneration observed in retinas of 4-week-old light-exposed *Rdh8*$^{-/-}$*Abca4*$^{-/-}$ mice. *OS*, outer segment; *IS*, inner segment; *ONL*, outer nuclear layer; *OPL*, outer plexiform layer; *INL*, inner nuclear layer; *IPL*, inner plexiform layer; *GCL*, ganglion cell layer. *Bars*, 20 μm.

them. For example, 11-*cis*-retinal is largely coupled to opsin or CRALBP, whereas all-*trans*-retinal is quickly removed from internal discs and reduced to the far less reactive all-*trans*-retinol. Visual cycle retinoids are sheltered from light of wavelengths shorter than ~400 nm, because the anterior eye filters it out. But this is no longer true when all-*trans*-retinal molecules condense to form products that absorb in the range of visible light. Upon excitation, their conjugated double bonds may be efficiently oxidized to form a variety of oxirane derivatives that trigger further radical reactions (32–34). If all-*trans*-retinal/*N*-retinylidene-phosphatidylethanolamine transfer by ABCA4 is slowed, A2PE and RALdi-PE conjugates would first accumulate inside the discs. Then with shedding and phagocytosis of ROS, the RPE could acquire excessive amounts of these products, as evidenced by accumulation of A2PE and RALdi-PE in the RPE from *Abca4*$^{-/-}$ mice (13) and humans with Stargardt disease (7).

Based on our results, it is reasonable to speculate that retinal degeneration in mice with delayed clearance of free all-*trans*-retinal is caused by several factors. Most likely RPE/photoreceptor cells tolerate high levels A2E and RALdi, but the additional presence of reactive compounds, most likely free all-*trans*-retinal, is detrimental for the eye. In such cases, profound and acute degeneration takes place. Additional animal models will be needed to confirm this hypothesis.

But is the retinopathy observed in *Rdh8*$^{-/-}$*Abca4*$^{-/-}$ mice causally related to abnormal retinoid metabolism or just an associated phenomenon? The dramatic effects of the retinoid cycle inhibitor retinylamine in protecting the retina against bright light-induced damage (Fig. 6) and delaying and ameliorating both A2E accumulation and retinal pathology (Fig. 7) argue strongly for a causal effect involving disrupted all-*trans*-retinal clearance. Importantly, the best therapeutic effects were obtained by pretreatment with retinylamine, and optimal protection was noted when therapy was initiated in the youngest animals (Fig. 7*E*). It should be noted that significant therapeutic effects also were observed when retinylamine was administered to mice with other etiologies of retinal degeneration (29, 30, 35).

Steps in Retinal Degeneration—Retinal degeneration in *Rdh8*$^{-/-}$*Abca4*$^{-/-}$ mice started as a punctuate process at the age of 4–6 weeks. These local changes correspond to the areas supported by single RPE cells, suggesting that retinal degeneration is promoted by death or impaired function of the RPE (Fig. 2*B*). By the age of 3 months, degeneration had progressed to the entire inferior retina and was accompanied by massive RPE death. Since retinal degeneration localized to the inferior region of the eye is characteristic of animal models with light-induced retinal damage and genetic alterations within the light-induced signaling cascade (15, 27, 30, 36), the unihemispherical distribution of retinal damage in *Rdh8*$^{-/-}$*Abca4*$^{-/-}$ mice strongly indicates that it also is associated with light exposure, and indeed, such damage was increased by light in *Rdh8*$^{-/-}$*Abca4*$^{-/-}$ mice (Fig. 6). Although pseudorosette formation might be promoted by different degenerative changes in a narrow area, acute induction of retinal degeneration by light exposure in *Rdh8*$^{-/-}$*Abca4*$^{-/-}$ mice well mimics the murine model of $NaIO_3$-induced punctuate RPE death and rosette formation (Fig. S1). These findings also indicate that the origin of this retinopathy primarily relates to the RPE, so we propose that aberrant reactions of the visual cycle are responsible for the initial insult to the retina.

Inhibition of the Visual Cycle and AMD—From the positive results in *Rdh8*$^{-/-}$*Abca4*$^{-/-}$ mice, we speculate that visual cycle inhibitors might not only provide optimal therapy for a juvenile macular degeneration called Stargardt disease, but also could be used to prevent disease progression in AMD. Recent

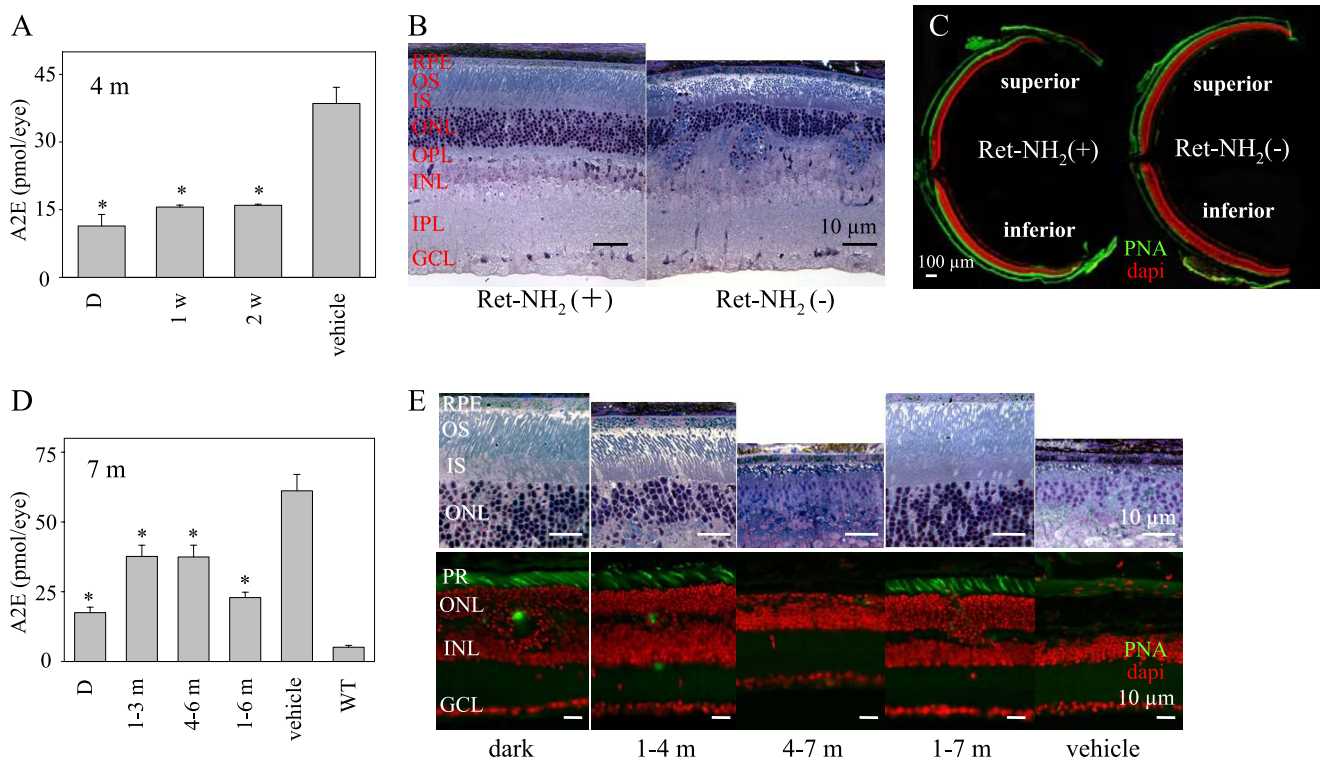

FIGURE 7. **Retinylamine treatment markedly reduces retinal degeneration in *Rdh8*$^{-/-}$*Abca4*$^{-/-}$ mice.** *A*, retinylamine (*Ret-NH*$_2$) treatment (1 mg given to 1-month-old mice by gastric gavage every week or every other week for 3 months) reduced A2E accumulation in *Rdh8*$^{-/-}$*Abca4*$^{-/-}$ mice kept in room light (less than 10 lux). A2E was quantified by reverse-phase HPLC. *X* axis, *D*, dark-reared; *1 w*, treated with retinylamine once per week; *2 w*, treated with retinylamine every other week; *vehicle*, treated with oil gavage every week. *Bars*, S.E. ($n > 6$; *, $p < 0.01$) *versus* vehicle-treated animals. *B*, retinylamine treatment every other week for 3 months, starting at 4 weeks of age, prevented retinal degeneration in *Rdh8*$^{-/-}$*Abca4*$^{-/-}$ mice examined 1 week after the last gavage. Retina from a vehicle-treated *Rdh8*$^{-/-}$*Abca4*$^{-/-}$ mouse shows retinal degeneration with retinal fold formation. *OS*, outer segment; *IS*, inner segment; *ONL*, outer nuclear layer; *OPL*, outer plexiform layer; *INL*, inner nuclear layer; *IPL*, inner plexiform layer; *GCL*, ganglion cell layer. *Bars*, 10 μm. *C*, 4-week-old *Rdh8*$^{-/-}$*Abca4*$^{-/-}$ mice treated with retinylamine every other week for 3 months did not show any retinal degeneration revealed by immunocytochemistry, whereas vehicle-treated animals developed severe degeneration of the inferior retina (*green*, PNA) cone stain; *red*, DAPI nuclear stain). Slides were prepared 1 week after the last gavage. *Bar*, 100 μm. *D*, effect of retinylamine treatments every other week for different periods on A2E accumulation in *Rdh8*$^{-/-}$*Abca4*$^{-/-}$ mice. A2E was quantified by reverse-phase HPLC. *X* axis, *D*, dark-reared; *1–3 m*, treated for 3 months starting at 1 month of age; *4–7 m*, treated for 3 months starting at 4 months of age; *1–7 m*, treated for 6 months starting at 1 month of age. Seven-month-old wild type mice received no treatment. *Bars*, S.E. ($n > 6$). *, $p < 0.01$ *versus* vehicle-treated animals. *E*, retinal histology of *Rdh8*$^{-/-}$*Abca4*$^{-/-}$ mice treated with retinylamine every other week for various periods. Treatment schedules were identical to those shown in *D*. *Top*, retinal histology of *Rdh8*$^{-/-}$*Abca4*$^{-/-}$ epon-embedded eyes. *Bottom*, cone photoreceptor and ONL changes as assessed by cryosection immunocytochemistry (*green*, PNA cone staining; *red*, DAPI nuclear staining). *Bars*, 10 μm. Retinylamine treatment for either 3 or 6 months and starting at 1 month of age largely prevented severe retinal degeneration, whereas 3 months of treatment starting at 4 months of age failed to do so.

research indicates that the risk of AMD development is enhanced by multiple factors, including genetic background, environmental effects, and immunological reactivity (37, 38). However, this work indicates that biochemical aberrations in cellular homeostasis can trigger changes leading to AMD. Evidence presented here indicates that combined deficiencies of RDH8 and ABCA4, resulting in delayed all-*trans*-retinal clearance and A2E accumulation, successfully reproduce key features of human AMD in a murine model. Although the *ABCA4* gene has been reported to modify AMD susceptibility in humans (39, 40), *Abca4*$^{-/-}$ mice failed to mimic human AMD (13). The *Rdh8*$^{-/-}$*Abca4*$^{-/-}$ mouse model, in contrast, presents several advantages over previously reported murine models. First, it reveals all of the major features of AMD, providing genetic proof that abnormal reactions of the visual cycle can cause progressive changes similar to AMD. Moreover, these changes occurred quite early (*i.e.* in the first 3 months of life). Different clinical phenotypes of dry type (atrophic) and wet type (exudative) human AMD might suggest that the pathogenesis of atrophic RPE/retina and choroidal neovascularization formation have different origins. However, our findings in *Rdh8*$^{-/-}$*Abca4*$^{-/-}$ mice provide strong evidence that dry and wet type phenotypes can both be induced by the same genetic defect.

Acknowledgments—We thank Drs. L. T. Webster (Case Western Reserve University), J. Nathans (Johns Hopkins University), and A. R. Moise (Case Western Reserve University) for comments on the manuscript; Dr. M. Hitomi (Case Western Reserve University) for help with electron microscopy; Dr. S. Sakami (Case Western Reserve University) for performing preliminary experiments; S. Roos and M. S. Matosky (Case Western Reserve University) for technical support; and Dr. R. S. Molday (University of British Columbia, Vancouver Canada) for providing anti-ABCA4 antibody.

REFERENCES

1. Travis, G. H., Golczak, M., Moise, A. R., and Palczewski, K. (2007) *Annu. Rev. Pharmacol. Toxicol.* **47,** 469–512
2. Palczewski, K. (2006) *Annu. Rev. Biochem.* **75,** 743–767
3. Filipek, S., Stenkamp, R. E., Teller, D. C., and Palczewski, K. (2003) *Annu.*

Rev. Physiol. **65,** 851–879
4. Molday, R. S. (2007) *J. Bioenerg. Biomembr.* **39,** 507–517
5. Rattner, A., Smallwood, P. M., and Nathans, J. (2000) *J. Biol. Chem.* **275,** 11034–11043
6. Parish, C. A., Hashimoto, M., Nakanishi, K., Dillon, J., and Sparrow, J. (1998) *Proc. Natl. Acad. Sci. U. S. A.* **95,** 14609–14613
7. Delori, F. C., Staurenghi, G., Arend, O., Dorey, C. K., Goger, D. G., and Weiter, J. J. (1995) *Investig. Ophthalmol. Vis. Sci.* **36,** 2327–2331
8. Fishkin, N. E., Sparrow, J. R., Allikmets, R., and Nakanishi, K. (2005) *Proc. Natl. Acad. Sci. U. S. A.* **102,** 7091–7096
9. Yannuzzi, L. A., Ober, M. D., Slakter, J. S., Spaide, R. F., Fisher, Y. L., Flower, R. W., and Rosen, R. (2004) *Am. J. Ophthalmol.* **137,** 511–524
10. Radu, R. A., Mata, N. L., Bagla, A., and Travis, G. H. (2004) *Proc. Natl. Acad. Sci. U. S. A.* **101,** 5928–5933
11. De, S., and Sakmar, T. P. (2002) *J. Gen. Physiol.* **120,** 147–157
12. Allikmets, R. (2000) *Am. J. Hum. Genet.* **67,** 487–491
13. Weng, J., Mata, N. L., Azarian, S. M., Tzekov, R. T., Birch, D. G., and Travis, G. H. (1999) *Cell* **98,** 13–23
14. Allikmets, R., Singh, N., Sun, H., Shroyer, N. F., Hutchinson, A., Chidambaram, A., Gerrard, B., Baird, L., Stauffer, D., Peiffer, A., Rattner, A., Smallwood, P., Li, Y., Anderson, K. L., Lewis, R. A., Nathans, J., Leppert, M., Dean, M., and Lupski, J. R. (1997) *Nat. Genet.* **15,** 236–246
15. Maeda, A., Maeda, T., Sun, W., Zhang, H., Baehr, W., and Palczewski, K. (2007) *Proc. Natl. Acad. Sci. U. S.A.* **104,** 19565–19570
16. Maeda, A., Maeda, T., Imanishi, Y., Kuksa, V., Alekseev, A., Bronson, J. D., Zhang, H., Zhu, L., Sun, W., Saperstein, D. A., Rieke, F., Baehr, W., and Palczewski, K. (2005) *J. Biol. Chem.* **280,** 18822–18832
17. Verdegem, P. J. E., Monnee, M. C. F., Mulder, P. P. J., and Lugtenburg, J. (1997) *Tetrahedron Lett.* **38,** 5355–5358
18. Golczak, M., Kuksa, V., Maeda, T., Moise, A. R., and Palczewski, K. (2005) *Proc. Natl. Acad. Sci. U. S. A.* **102,** 8162–8167
19. Chen, Y., Hu, Y., Lu, K., Flannery, J. G., and Ma, J. X. (2007) *J. Biol. Chem.* **282,** 34420–34428
20. Kim, S. R., Jang, Y. P., Jockusch, S., Fishkin, N. E., Turro, N. J., and Sparrow, J. R. (2007) *Proc. Natl. Acad. Sci. U. S. A.* **104,** 19273–19278
21. Wenzel, A., Reme, C. E., Williams, T. P., Hafezi, F., and Grimm, C. (2001) *J. Neurosci.* **21,** 53–58
22. Kim, S. R., Fishkin, N., Kong, J., Nakanishi, K., Allikmets, R., and Sparrow, J. R. (2004) *Proc. Natl. Acad. Sci. U. S. A.* **101,** 11668–11672
23. Eldred, G. E. (1993) *Nature* **364,** 396
24. Rattner, A., and Nathans, J. (2006) *Nat. Rev.* **7,** 860–872
25. Evans, J. R. (2001) *Prog. Retin. Eye Res.* **20,** 227–253
26. Sparrow, J. R., Nakanishi, K., and Parish, C. A. (2000) *Investig. Ophthalmol. Vis. Sci.* **41,** 1981–1989
27. Nilsson, S. E., Knave, B., and Persson, H. E. (1977) *Acta Ophthalmol.* **55,** 994–1006
28. Mata, N. L., Tzekov, R. T., Liu, X., Weng, J., Birch, D. G., and Travis, G. H. (2001) *Investig. Ophthalmol. Vis. Sci.* **42,** 1685–1690
29. Golczak, M., Maeda, A., Bereta, G., Maeda, T., Kiser, P. D., Hunzelmann, S., von Lintig, J., Blaner, W. S., and Palczewski, K. (2008) *J. Biol. Chem.* **283,** 9543–9554
30. Maeda, A., Maeda, T., Golczak, M., Imanishi, Y., Leahy, P., Kubota, R., and Palczewski, K. (2006) *Mol. Pharmacol.* **70,** 1220–1229
31. Golczak, M., Imanishi, Y., Kuksa, V., Maeda, T., Kubota, R., and Palczewski, K. (2005) *J. Biol. Chem.* **280,** 42263–42273
32. Ben-Shabat, S., Parish, C. A., Vollmer, H. R., Itagaki, Y., Fishkin, N., Nakanishi, K., and Sparrow, J. R. (2002) *J. Biol. Chem.* **277,** 7183–7190
33. Liu, J., Itagaki, Y., Ben-Shabat, S., Nakanishi, K., and Sparrow, J. R. (2000) *J. Biol. Chem.* **275,** 29354–29360
34. Ben-Shabat, S., Itagaki, Y., Jockusch, S., Sparrow, J. R., Turro, N. J., and Nakanishi, K. (2002) *Angew. Chemie Int. Ed. Engl.* **41,** 814–817
35. Maeda, A., Maeda, T., and Palczewski, K. (2006) *Invest. Ophthalmol. Vis. Sci.* **47,** 4540–4546
36. Chen, J., Simon, M. I., Matthes, M. T., Yasumura, D., and LaVail, M. M. (1999) *Investig. Ophthalmol. Vis. Sci.* **40,** 2978–2982
37. Haines, J. L., Spencer, K. M., and Pericak-Vance, M. A. (2007) *Proc. Natl. Acad. Sci. U. S. A.* **104,** 16725–16726
38. Hollyfield, J. G., Bonilha, V. L., Rayborn, M. E., Yang, X., Shadrach, K. G., Lu, L., Ufret, R. L., Salomon, R. G., and Perez, V. L. (2008) *Nat. Med.* **14,** 194–198
39. Allikmets, R., Shroyer, N. F., Singh, N., Seddon, J. M., Lewis, R. A., Bernstein, P. S., Peiffer, A., Zabriskie, N. A., Li, Y., Hutchinson, A., Dean, M., Lupski, J. R., and Leppert, M. (1997) *Science* **277,** 1805–1807
40. Shroyer, N. F., Lewis, R. A., Yatsenko, A. N., Wensel, T. G., and Lupski, J. R. (2001) *Hum. Mol. Genet.* **10,** 2671–2678